High Payload Capacity for Fully Autonomous Battery-Powered Flying Artificial Insects

By Francisco Gonçalves (WSU), Ryan M. Bena (USC), and Néstor O. Pérez-Arancibia (WSU)

1. Abstract

Regardless of the source of power, in order for artificial insects to achieve full autonomy from the energy perspective, both their payload capacities and maneuver abilities must be optimized. To that end, in 2019, at the autonomous microrobotic systems laboratory (AMSL), we introduced a new 95-mg four-wing four-actuator flapping-wing flying microrobot, the Bee+. This robot showed significant promise as its robotic design enabled us to solve the long-standing problem of yaw-angle control; however, its recorded maximum thrust-to-weight ratio was similar to that achieved by the original Harvard RoboBee. In this poster, we present a new version of the Bee+, the Bee++ [1], which has been shown to perform high-speed aerobatic maneuvers with a maximum thrust-to-weight ratio in the order of 3.9 at high flapping frequencies (> 160 Hz). This figure represents a significant step forward in the quest toward achieving full autonomy, from both the power and control perspectives, at the subgram scale because the resulting payload capacity is sufficiently large to carry all the power electronics, computation, sensing, and energy systems required for autonomous flight for a few minutes.

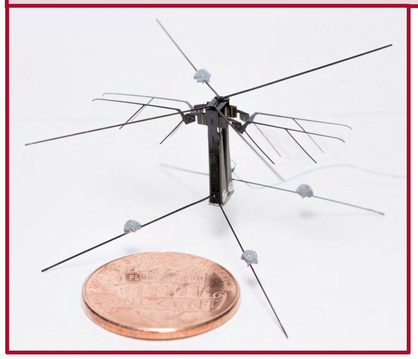

A Bee++ prototype next to a US penny. This robot weighs 95 mg and has a wingspan of 33 mm. Before performing flight experiments, thin carbon fiber spars and reflective markers, which in total weigh about 5mg, are attached to the robots. The spars provide collision protection and support the reflective markers that are used by a Vicon motion capture system to track the positions and attitudes of the tested Flapping-Wing Micro Air Vehicles (FWMAVs).

2. Microscale design & Energy, and Power Challenges

2. 1. Robotic Design of the Bee++

The four-wing four-actuator design of the Bee++ allows independent drive of its four wings, therefore increasing the control authority of the system when compared to two-wing robots like the Harvard RoboBee. The two pairs of twinned unimorph actuators together with a preset inclination with respect to the plane defined by the leading edges of the four composing wings while at rest give the Bee++ the ability to produce body-yaw torques, thus improving the yaw controllability of the robot [1].

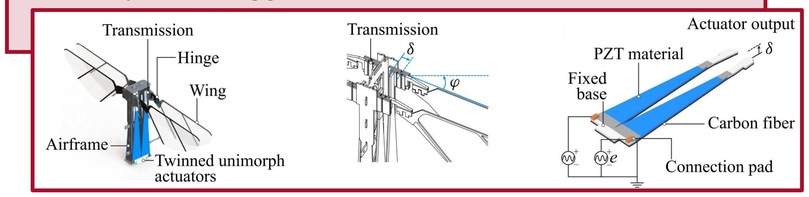

Bee++ design with an overview of the four-wing four-actuator design, the transmission mechanism used, and an illustration of a pair of twinned unimorph actuators used to drive two of the four wings of a Bee++ prototype.

2. 2. Power in microrobotics

Powering microrobots is a problem for which an optimal solution has not yet been found, and therefore, it is an area with large room for research and improvement. Since the mass of the lightest high power density batteries is currently in the order of magnitude around $10^1 \sim 10^2\ mg$, the maximum thrust-to-weight ratio shown by the Bee++ (3.9) would be enough to support them, thus moving a step forward on enabling fully-autonomous FWMAVs.
Although these batteries can still only provide few minutes of autonomous flight, those minutes can be leveraged to go from a charging point to another, and that way, increase the total flight duration.

2. 3. How would a current lightweight battery perform on Bee++?

- 140 mg battery presented in [2]
- Bee++ consumes 50 ~ 150 mW which corresponds approximately to 3 to 5 minutes of flying time according to the discharge power graph
- Trade-off must be made between Energy and Power Densities

(a) 140 mg high power density battery [2].
(b) Discharge power as a function of time [2].

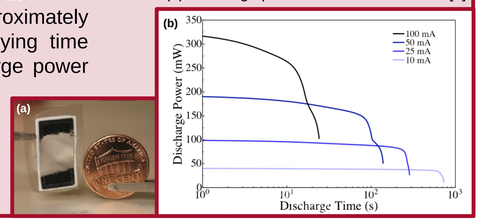

3. Controller Design

3. 1. Dynamic Modeling of the Flying Microrobot

- Inertial frame, $\mathcal{N}$: $\{\mathcal{O}_0, \boldsymbol{n_1}, \boldsymbol{n_2}, \boldsymbol{n_3}\}$.
- Body-fixed frame, $\mathcal{B}$: $\{\mathcal{O}_\mathcal{B}, \boldsymbol{b_1}, \boldsymbol{b_2}, \boldsymbol{b_3}\}$.

Note that the vectors $\boldsymbol{b_1}$, $\boldsymbol{b_2}$, and $\boldsymbol{b_3}$ correspond to the roll, pitch, and yaw axes of the modeled robotic flyer.

Translational and Rotational Dynamics

$$\dot{\boldsymbol{r}} = \boldsymbol{v}$$

$$\dot{\boldsymbol{v}} = \frac{f}{m}\boldsymbol{b}_3 - g\boldsymbol{n}_3$$

$$\dot{\boldsymbol{q}} = \frac{1}{2}\boldsymbol{q} \otimes \begin{bmatrix} 0 \\ \boldsymbol{\omega} \end{bmatrix}$$

$$\dot{\boldsymbol{\omega}} = \boldsymbol{J}^{-1}(\boldsymbol{\tau} - \boldsymbol{\omega} \times \boldsymbol{J}\boldsymbol{\omega})$$

where $\boldsymbol{v}$ denotes the velocity of the robot's COM relative to $\boldsymbol{\mathcal{O}_0}$.

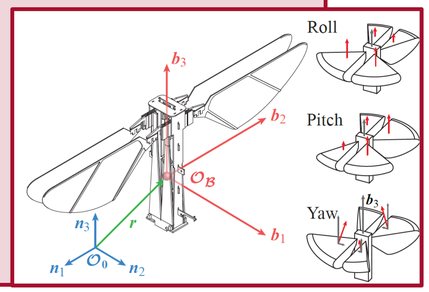

Bee++ Design and Flapping motions for different rotations

3. 2. Position Controller

$$\boldsymbol{f}_a(t) = \boldsymbol{K}_p[\boldsymbol{r}_d(t) - \boldsymbol{r}(t)] + \boldsymbol{K}_i \int_0^t [\boldsymbol{r}_d(\tau) - \boldsymbol{r}(\tau)]d\tau + \boldsymbol{K}_d[\dot{\boldsymbol{r}}_d(t) - \dot{\boldsymbol{r}}(t)] + m\ddot{\boldsymbol{r}}_d(t) + mg\boldsymbol{n}_3$$

$$b_{d,3} = \frac{\boldsymbol{f}_a}{\|\boldsymbol{f}_a\|_2}$$

$$b_{d,1} = \frac{[-\sin\psi_d \ -\cos\psi_d \ 0]^T \times b_{d,3}}{\|[-\sin\psi_d \ -\cos\psi_d \ 0]^T \times b_{d,3}\|_2}$$

$$b_{d,2} = b_{d,3} \times b_{d,1}$$

In the configuration shown below, $\boldsymbol{r}_d$ and $\boldsymbol{r}$ are the reference and measured position signals with respect to $\mathcal{N}$, respectively. The outputs generated by the position controller are the magnitude of the total thrust command, f, and the desired attitude quaternion, $\boldsymbol{q}_d$. To generate the control signal, first, the algorithm computes the instantaneous thrust-force vector written with respect to the inertial frame, f_a, required to compel the robot to track a desired trajectory, according to the LTI law shown above, where $\boldsymbol{K}_p$, $\boldsymbol{K}_i$, and $\boldsymbol{K}_d$ are diagonal positive-definite gain matrices.

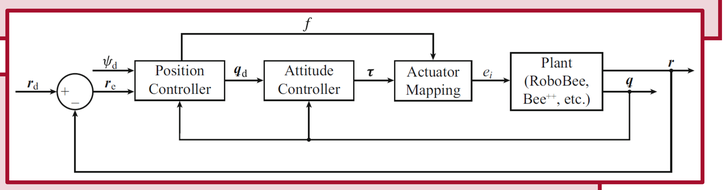

3. 3. Attitude Controller

$$\boldsymbol{q}_e = \boldsymbol{q}^{-1} \otimes \boldsymbol{q}_d$$

$$\begin{bmatrix} 0 \\ \boldsymbol{\omega} \end{bmatrix} = 2\dot{\boldsymbol{q}}^{-1} \otimes \boldsymbol{q}$$

$$\begin{bmatrix} 0 \\ \hat{\boldsymbol{\omega}}_d \end{bmatrix} = 2\dot{\boldsymbol{q}}_d{}^{-1} \otimes \boldsymbol{q}_d$$

$$\boldsymbol{\omega}_d = \boldsymbol{S}^T \boldsymbol{S}_d \hat{\boldsymbol{\omega}}_d$$

With $\boldsymbol{q_d}$ and $\boldsymbol{q}$, that represents the current measured attitude of the body-fixed frame with respect to the inertial frame, the attitude controller computes the attitude-error quaternion, representing the attitude of the desired frame of reference relative to the body-fixed frame. In this quaternion, the direction of the vector $\boldsymbol{n_e}$ is particularly important since it represents the Euler rotation axis between the body-fixed frame and the desired frame of reference. Finally, the controller calculates the torque in body-fixed coordinates required to make the robot to track the desired attitude, specified by the quaternion $\boldsymbol{q_d}$, using the LTI feedback law below.

$$\boldsymbol{\tau} = \boldsymbol{K}_q \boldsymbol{n}_e + \boldsymbol{K}_\omega(\boldsymbol{\omega_d} - \boldsymbol{\omega}) + \boldsymbol{J}\dot{\boldsymbol{\omega}}_d + \boldsymbol{\omega} \times \boldsymbol{J}\boldsymbol{\omega}$$

5. Bee++ Flight Tests

Here, we present the results obtained through a single representative flight test that, in general, is highly repeatable, and the measured response can be considered typical in terms of performance and stability robustness. The robot starts its trajectory from $r = [0\ 0\ 0]^T\ m$ and then follows the position reference $\boldsymbol{r}_d(t)$, for $t \in [0{:}\ 20]\ s$. During those 20 s the Bee++ prototype successfully took off, stably tracked a constant altitude-position reference ($\boldsymbol{r}_d = [0\ 0\ 0.15]^T\ m$) and performed a controlled landing maneuver.

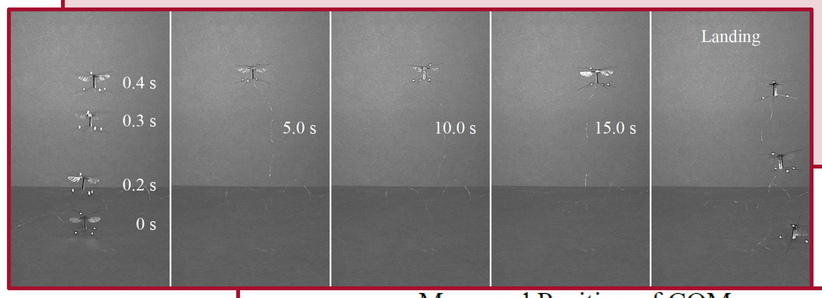

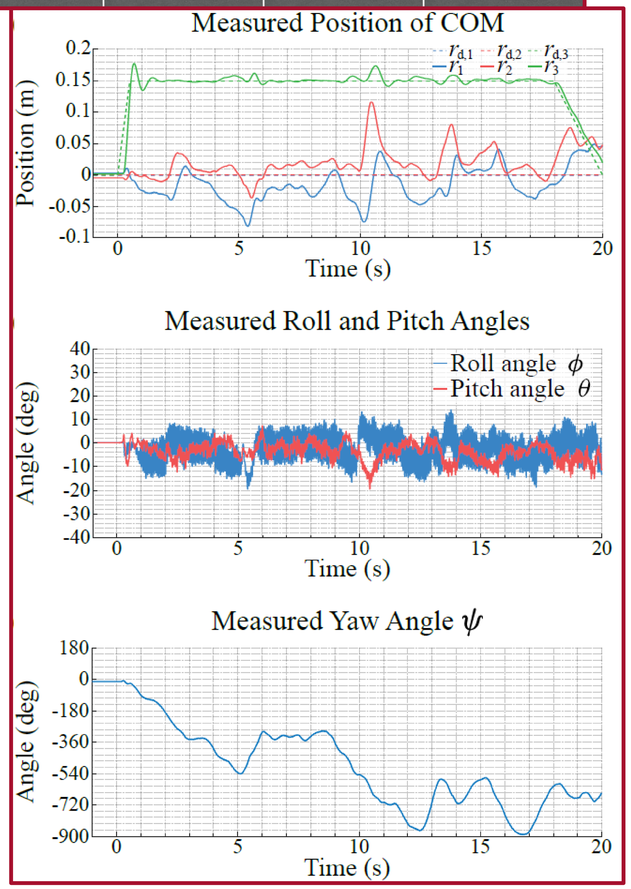

References

[1] Bena, R.M., Nguyen, XT., Yang, X. *et al.* A Multiplatform Position Control Scheme for Flying Robotic Insects. *J Intell Robot Syst* **105,** 19 (2022). https://doi.org/10.1007/s10846-021-01556-2
[2] Duduta, Mihai et al. "Ultra-Lightweight, High Power Density Lithium-Ion Batteries." *Batteries & Supercaps* (2018): n. pag.